

# Lithographic Performance in Thick Photoresist Applications

by

Gary E. Flores, Warren W. Flack, Elizabeth Tai  
Ultratech Stepper, Inc.  
Santa Clara, CA

Chris A. Mack  
FINLE Technologies  
Austin, TX

## AUTHOR BIOGRAPHIES

*Gary E. Flores is a senior applications engineer at Ultratech Stepper where he is responsible for application support and development of lithography stepper processes. He received his BS degree in Chemical Engineering from the University of California at Berkeley in 1983 and MS degree from the University of California at Santa Barbara in 1985. Prior to joining Ultratech Stepper, he was employed with KTI Chemicals, Inc. as a senior technical development engineer, where he worked on the development of lithographic materials and processes. From 1985 through 1990 he worked at TRW's Microelectronics Center as a senior process engineer, with responsibilities in optical lithography, dry etching and wet etching.*

*Warren W. Flack is the Asian applications manager for Ultratech Stepper based out of Tokyo, Japan. He is responsible for customer applications support for thin film head and silicon semiconductor applications. Before joining Ultratech Stepper in 1992, he was senior section head for pattern transfer at TRW's Microelectronics Center. There he was responsible for optical lithography, electron-beam lithography and dry etching for advanced silicon technologies. He received his BS and MS degrees in Chemical Engineering from the Georgia Institute of Technology in 1978 and 1979 and his PhD in Chemical Engineering from the University of California at Berkeley in 1983.*

*Elizabeth Tai is a senior process development engineer at Ultratech Stepper. She has over 10 years experience in the characterization of lithographic processes for manufacturing and customer applications. Before joining Ultratech Stepper in 1987, she was a senior process engineer at Micronix where she was involved in the development of experimental x-ray and e-beam resists and multilayer resist schemes for x-ray lithography. She received her bachelor's degree from New York University in molecular biology.*

*Chris A. Mack received Bachelor of Science degrees in Physics, Chemistry, Electrical Engineering and Chemical Engineering from Rose-Hulman Institute of Technology in 1982 and a Master of Science degree in Electrical Engineering from the University of Maryland in 1989. He joined the Microelectronics Research Laboratory of the Department of Defense in 1983 and began work in optical lithography research. He has authored numerous papers*

*in the area of optical lithography, regularly teaches courses on this topic, and has developed the lithography simulation programs PROLITH and PROLITH/2. During 1990-1991 he was on assignment at SEMATECH working in deep-UV photoresist characterization and phase-shifting optimization. Since January of 1992 he has been Vice President of Research and Development for FINLE Technologies and also serves as an adjunct faculty at the University of Texas at Austin.*

## **ABSTRACT**

Thin film head devices used for magnetic read/write technology have become a major driving force for advances in high performance data storage systems, such as high capacity hard disk drives. These thin film heads (TFH) are produced using planer technologies similar to integrated circuit (IC) manufacturing. The lithography processes inherent in the manufacturing of TFH devices provide unparalleled challenges due to a number of process factors: photoresist thickness as thick as 40 microns, topography as large as 20 microns, extreme substrate reflectivities from metal plating processes and image aspect ratios as large as 6:1. These challenges, although different than those for submicron lithography, are of comparable difficulty. And unlike thin photoresist applications for IC manufacturing, which typically use less than two micron films, lithographic modeling and characterization has been limited for thick film applications. This study elucidates some of the photoresist properties required for successful lithography in thick photoresist materials. This includes issues with conventional models for development of a polymer film which are inadequate for thick photoresists due to an observed developer macro/micro disparity. This is speculated to be due to developer loading effects and polymer dissolution kinetics. Another concern is the optical transparency of the photoresist film, where increasing film thickness can have profound effects on lithographic performance due to bulk and interference effects.

The performance of several commercially available photoresists is examined to gain insight into the effects optical and dissolution properties have on industry standard process metrics. This includes examining how small changes in photoresist properties are manifested in these process metrics. The impact of increasing film thickness is characterized for bulk development properties, exposure latitude, sidewall angle, focus latitude, exposure sensitivity, and develop time. The adequacy of lithographic models is determined by comparison of experimental results to simulation predictions. The tradeoffs between various parameters is reviewed and compared to process requirements for thin film head lithography.

## **INTRODUCTION**

Advances in computers systems are typically associated with new generation microprocessors and higher densities of dynamic access memory (DRAM) circuits. However, the performance of computers is also critically dependent on the associated mass storage systems. These systems are typically high capacity hard disk drives which provide rapid access to stored data. Manufacturers are requiring smaller and faster hard drives for new computer designs. The disk drive storage

capacity per unit of platter area can be increased by improvements in magnetic recording media and read/write head technologies [1]. Extensive effort has been directed in the enhancement of read/write heads because it offers the largest potential for rapid improvements. Advanced read/write heads are manufactured on ceramic substrates using planer technologies similar to semiconductor devices, and this class of devices is referred to as thin film heads (TFH).

Most current generation TFH designs use inductive techniques for both reading and writing on the magnetic media. An electric current is passed through a copper coil which induces a magnetic flux in the gap between permalloy poles as shown in figure one. Reversing the current provides the necessary orientation factor for binary storage of individual bits of data [2]. Overall data storage can be increased by TFH improvements in two areas: higher linear bit density and reduction of the track width of the head. The linear density is dependent on the width of the gap between the poles. Reducing the gap allows more bits per unit length of track. Reducing the track width allows more tracks to be recorded per inch [2]. However, more copper coils are required to read the state of the magnetic media when the individual transition region becomes smaller. The increased coil capacity is typically obtained by fabricating as many as four coil levels in the TFH, which increases the total structure height [3]. This can cause TFH elements to rise 20 to 30 microns above the substrate surface creating large steps which must be covered with photoresist during lithographic processing [1].

The performance of a TFH can be increased by using a magnetoresistive (MR) head for reading and an inductive head for writing. The MR head applies a constant current and measures the resulting change in voltage as a function of substrate magnetization [2]. The increased sensitivity of the MR head allows a reduction in the number of copper coils required for the inductive head, which is then only required for writing. However, the MR head adds substantial process complexity because it must be incorporated with the inductive head. The relative placement of the write element and the read element is important to prevent head tracking problems [4].

Many of the critical issues for TFH fabrication are directly related to the lithography process. Critical dimension (CD) control for the copper coils and the top and bottom poles are important for TFH performance. However, the large topography present in the typical head requires the use of photoresist films over 10 microns thick with associated large expose doses. This results in a loss of control in linewidth due to variations in photoresist thickness in excess of 50% in the area of a large step [5]. Slopes in a thick photoresist film also reduce the CD control. The bulk effect of the photoresist reduces the effective dose at the bottom of the film and combines with the isotropic wet development process to produce sloped profiles [5]. An additional factor which impacts CD control is the high reflectivity of the plated metal films which can result in standing wave phenomena.

Another lithographic issue is alignment of the TFH structures [5]. The alignment of the top and bottom pole determines the ultimate track density and therefore the areal density of a given disk drive as shown in figure two. This alignment step is challenging because of the large steps heights involved and the requirement to align through a thick photoresist film. Another critical

alignment is the MR head relative to the write inductive head. If the alignment is not well controlled, there will be a tracking error between the heads which reduces the areal density.

The semiconductor industry has made extensive use of lithography process modeling to reduce required experimental work and to obtain a better fundamental understanding of complex problems. For example, broadband i-line lithography [6] and deep UV excimer lithography [7] have been modeled using the simulation package PROLITH/2<sup>®</sup>. These semiconductor processes involve substantially smaller geometries and thinner photoresist films than TFH processes. However, the photoresist height to linewidth aspect ratios for the TFH process are actually larger than those in the semiconductor industry, suggesting the lithographic problems are just as challenging. Clearly, TFH lithography could benefit from process modeling for the same reasons it is used in semiconductor processes.

Photoresist dissolution has been extensively studied for thin film photoresist applications [8]. However, it is not clear that the existing thin film models will be adequate to describe the behavior of the thick photoresist films used for TFH. The purpose of this study is to experimentally evaluate commercially available photoresists and compare the resulting industry standard metrics to the model results. The effects of various modeling parameters were evaluated to determine how photoresist materials could be improved for TFH applications in the future.

## PROCESS SIMULATION

Process simulation and modeling techniques have demonstrated significant success in predicting the behavior of optical lithography for semiconductor processes with photoresist thicknesses below two microns. An extension of these same principles and methods can be applied to the lithographic processes for TFH technology. This approach can provide tremendous insight into the crucial photoresist properties that are needed for successful process requirements in TFH applications. The lithography simulator PROLITH/2<sup>®</sup>, a second generation optical lithography model, was used for all calculation activities in this work. The imaging system modeled is a Ultratech Stepper 1700, which was specifically designed for TFH lithographic applications.

### Factorial Simulation Experiment

An effective and efficient approach to characterizing multi-factor systems is the use of experimental design methodologies [9]. For this study, three photoresist model parameters were varied in a full factorial design scheme. These are the photoresist absorption parameter  $\mathbf{A}$  ( $\mu\text{m}^{-1}$ ) and two develop model parameters: the developer selectivity  $\mathbf{n}$ , and the maximum development rate  $\mathbf{R}_{\text{max}}$  (nm/sec) from the Mack develop model [10]. The corresponding low and high values are listed in table 1. The ranges were selected to correspond to typical values encountered in high contrast g-line photoresists. This scheme allowed a series of theoretical photoresists to be examined to analyze the effects of different parameters. A total of eight unique simulation trials were run, where each trial was a focus/exposure matrix characterization of both photoresist critical dimension (spacewidth) and sidewall angle. The remaining modeling parameters were

assigned as shown in table 2. These settings were based on the lithography system, substrate type and standard photoresist properties.

As previously noted for TFH processing, a particularly crucial lithography process level is the top pole. Typically this level requires patterning a 4 to 6 micron spacewidth in a 10 micron thick photoresist film. The complexity of this level is exacerbated by the extreme topography which is encountered. For this level, a depth-of-focus window of approximately 16 microns is desirable. This requirement is driven by photoresist thickness coating variations, severe topography, substrate flatness and focus system imprecision due to the severely varied substrate topography.

In order to study the focus window for a 16 microns depth-of-focus process, three separate defocus conditions were examined: -3.3 microns, -11.3 microns and 4.7 microns. The -3.3 micron defocus corresponds to the isofocal point for a 10 micron film, or a focus 1/3 of the distance into the film. The remaining focus settings of -11.3 and 4.7 were then selected symmetrically around the isofocal setting. Expose ranges for the focus/exposure matrix were varied from 200 to 3000 mJ in either 50 or 100 mJ increments. These conditions provided a broad view of the process window at each unique photoresist condition.

The required exposure dose to achieve a nominal mask spacewidth of 4.0 microns (dose to size) was determined for each simulation at the -3.3 micron defocus, which will be shown to represent best focus. Figures 3 and 4 display contour plots of the behavior of dose to size as a function of  $\mathbf{A}$  and  $\mathbf{n}$  for the two conditions of  $\mathbf{R}_{\max}$  equal to 50 and 200 nm/sec respectively. In both cases, it is evident that increasing  $\mathbf{A}$  and increasing  $\mathbf{n}$  result in larger dose to size values. For the extreme conditions of  $\mathbf{A}$  equal to 1.1 and  $\mathbf{n}$  equal to 6.0, dose to size requirements are in the 2000 mJ/cm<sup>2</sup> range, which is a four fold increase from the 250 mJ/cm<sup>2</sup> requirement where  $\mathbf{A}$  is 0.4 and  $\mathbf{n}$  is 1.5. However, a comparison of figures 3 and 4 reveals the impact of  $\mathbf{R}_{\max}$  is less important with both contour surfaces appearing similar.

Four additional process response metrics were used for optimizing the photoresist factors studied in the factorial design:

1. Exposure latitude -3.3 microns defocus
2. Sidewall angle -3.3 microns defocus
3. Exposure latitude -11.3 microns defocus
4. Sidewall angle -11.3 microns defocus.

These results are summarized in table 3. Note that exposure latitude was defined using a  $\pm 10\%$  spacewidth criteria (3.6 to 4.4 microns) for each trial. Sidewall angle responses are based on conditions of dose to size.

Exposure process latitude and sidewall angle are maximized at the process conditions where  $\mathbf{A}$  is 0.4,  $\mathbf{n}$  is 6.0 and  $\mathbf{R}_{\max}$  is 200 at either focus setting. It is clear that the poorest exposure latitude and lowest sidewall angle occurs where  $\mathbf{A}$  is 0.4 and  $\mathbf{n}$  is 1.5 for both  $\mathbf{R}_{\max}$  values. All the

conditions where  $A$  equals 1.1 have comparable exposure latitude in the range of 81 to 100% and sidewall angles of 83 to 86 degrees at -3.3 microns defocus.

It is also useful to look at spacewidth as a function of normalized exposure for a range of focus settings. Normalized exposure dose was defined as exposure dose divided by dose to size at -3.3 microns defocus. The development times are proportional to the photoresist thickness using the relationship specified in table 2. Figure 5 displays three extreme conditions of the factorial design space:

(a) Minimum latitude	$A = 0.4$	$n = 1.5$	$R_{\max} = 50$
(b) Maximum latitude	$A = 0.4$	$n = 6.0$	$R_{\max} = 200$
(c) Maximum values	$A = 1.1$	$n = 6.0$	$R_{\max} = 200$

which are shown in figures 5(a), 5(b) and 5(c) respectively. A comparison of Figures 5(a) and 5(b) reveals that increasing the developer selectivity  $n$  from 1.5 to 6.0 and  $R_{\max}$  from 50 to 200 improves the exposure latitude and the focus latitude over the 16 micron focus range. It is also apparent that at the low value of  $n$ , the spacewidth control at nominal exposure conditions is limited. This suggests that improved spacewidth control occurs during overexposed conditions (25% above normalized exposure), but this requires a size bias in excess of 0.5 microns. These bias effects are reduced with the increase in  $n$  to 6.0 and  $R_{\max}$  to 200. The impact of increasing the  $A$  value from 0.4 to 1.1 can be seen by comparing figures 5(b) and 5(c). While comparable exposure latitude occurs for these conditions, it should be noted that there is a large penalty in exposure dose (750 versus 2400 mJ/cm<sup>2</sup>). A general feature of all the normalized plots is the best exposure latitude is at -3.3 microns defocus and poorest exposure latitude is at -11.3 microns defocus.

Sidewall angle profiles for minimum latitude, maximum latitude and maximum values are shown in figures 6(a), 6(b) and 6(c) respectively. As was seen for exposure latitude in figure 5, the focus setting of -3.3 microns provides the highest sidewall angle. These results offer further support for the ranking of the three process conditions from figure 5. Again, inferior performance occurs for  $A$  equal to 0.4,  $n$  equal to 1.5 and  $R_{\max}$  equal to 50. Figure 6(c) shows an interesting enhancement of sidewall angle with overexposure for -3.3 microns defocus. In contrast, the defocus settings of -11.3 and 4.7 microns are relatively flat at 82 and 78 degrees. These values are nearly similar to the defocus conditions for figure 6(b).

### Photoresist Thickness Effects

TFH processes require the use of a broad range of photoresist thicknesses due to the variety of topography encountered during manufacturing. In order to determine the effect of thickness on lithographic performance, photoresist thicknesses of 2, 5, 10 and 20 microns were examined at the conditions  $A$  equal to 0.4,  $n$  equal to 6.0 and  $R_{\max}$  equal to 200.

Figure 7 shows spacewidth as a function of normalized exposure at the isofocal condition for each photoresist thickness. It is interesting to note that the 2, 5 and 10 micron thicknesses show very similar results. However, the 20 micron photoresist shows a much smaller process window. This suggests that bulk film effects may be playing a significant role in this very thick photoresist film. Similarly, sidewall angle profiles as a function of normalized exposure are shown in figure 8. It is apparent that there is a degradation in sidewall angle with increasing photoresist thickness. This would be expected due to developer loading effects and the optical transparency of the thick films.

## **EXPERIMENTAL PROCEDURES**

Two commercially available photoresist products, Hoechst Celanese AZ 4000 and Shipley STR 1000 were examined for their develop rate behavior, focus/exposure process windows and photoresist profiles. Both materials are specifically designed for thick photoresist applications. A high viscosity formulation of the AZ series, P 4620, was used for studying the 5 and 10 micron thickness regimes while P 4110 was used for 2 micron processes. A high viscosity formulation of the STR series, 1075 (44% solids) was used for 10 micron thickness regime, 1045 (38% solids) was used for the 5 micron regime and XP 90190 (21% solids) was used for the 2 micron processes.

An Ultratech Stepper model 1500 was used for all experiments. The projection optics are based on the Wynne-Dyson-Hershel 1x lens design, with broadband illumination of the g and h mercury lines including the continuum from 390 to 450 nm. This system supports both a variable NA and partial coherence capability. A numerical aperture of 0.24 and partial coherence of 0.85 was used for all tests.

The photoresist coat and softbake processes were performed on an Solitec 5110C track system. Static dispense techniques were used for all photoresist coating applications. Note that the spin time, acceleration and spin speed were intentionally varied in the experimental designs to achieve the desired film thickness.

Softbake processing was performed on either a Blue M convection oven or a MTI Flexifab hot plate bake system. For the AZ photoresist, a 105° C 45 minute convection bake was used while the Shipley STR used a 100° C 90 second hot plate bake.

Photoresist development processing was performed using a batch immersion method with constant agitation at room temperature. The AZ 4000 series photoresist was developed using AZ 400K developer mixed in a 5:1 ratio with dionized (DI) water, which provided a 0.23 N solution. The Shipley STR 1000 series photoresist was developed using premixed Shipley 452 developer.

## EXPERIMENTAL RESULTS

### Develop Rate Results

The develop rate characteristics for the two families of photoresists were measured at 2, 5 and 10 micron thicknesses. Develop rate data was determined using standard open frame dose clear methods (contrast curves). A range of 50 to 650 mJ/cm<sup>2</sup> exposures in 15 mJ increments were used for each case. This range of exposures was repeated for a matrix of develop times. For the 2 micron film thicknesses, develop times of 1 to 4 minutes in half minute steps were performed. Develop times of 2, 2.5, 3, 3.5, 4, 4.5, 5, 6 and 8 minutes were performed for the 5 micron photoresist thicknesses, while develop times of 3, 4, 5, 6, 7, 8, 9, 10 and 12 minutes were used for the 10 micron photoresists. Resulting film thicknesses were measured using an Alpha step stylus profilometer.

Photoresist develop rates were then calculated for each exposure energy from film thickness versus develop time rate curves. This provided an effective average develop rate for a given film thickness and exposure dose. A corresponding average Photo Active Compound (PAC) concentration was then determined for the various exposure energies and film thicknesses. Photoresist development rate versus relative PAC is shown in figures 9 and 10 for the AZ 4000 family and Shipley STR 1000 family photoresists respectively. Initial film thicknesses of 2, 5 and 10 microns are shown in graphs (a), (b) and (c) respectively.

The develop rate model proposed by Trefonas and Mack was fit to the experimental data shown in figures 9 and 10 [10]:

$$\text{Rate} = R_{\max} (1 - e^{-EC})^n + R_{\min} \quad (1)$$

where  $R_{\max}$  is the maximum develop rate of fully exposed photoresist,  $R_{\min}$  is the unexposed develop rate,  $n$  is the developer selectivity,  $E$  is the exposure dose and  $C$  is the effective photoresist rate constant. The term  $e^{-EC}$  is equivalent to the relative PAC concentration [10], hence equation (1) can be fit to the experimental results to determine the develop rate parameters.

The develop rate parameters determined from the regression analysis are shown for each photoresist thickness next to the individual graphs in figures 9 and 10. For the AZ 4000 family of photoresists, the experimentally determined  $R_{\max}$  values were found to be on the order of 30 to 60 nm/sec. The value for the STR 1000 family was slightly higher around 60 to 75 nm/sec. Note that the exposure doses used in the experiment did not fully encompass high PAC conversion for the thicker photoresist case of 10 microns. One clear trend of the develop rate behavior with increasing film thickness is an apparent steepening of the rate versus relative PAC concentration.

One of the large differences between the two photoresist products is the  $n$  value. The STR 1000 family shows  $n$  values of approximately 4.5 to 5.0 while the AZ 4000 family has  $n$  values around 1.2 to 2.5. Based on the factorial simulation experiments, the higher  $n$  values of the STR 1000

family should provide enhanced exposure latitude and focus latitude compared to the AZ 4000 family.

### **Focus/Exposure Results**

Cross sectional SEM analysis was used to evaluate the quality of 4 micron line and space patterns in 10 microns of photoresist as a function of focus. The results for AZ P 4620 and STR 1075 are shown in figures 11 and 12 respectively. It is apparent that the STR 1075 shows better CD control over a larger range of focus than the AZ P 4620. This is not surprising considering the differences in **n** values determined for STR 1075 and AZ P 4620 in the previous develop rate analysis. It is interesting to note that both photoresists show a “milk bottle” profile for large negative defocus. This confirms the model simulations that a large negative defocus should have the poorest exposure latitude.

Complete SEM analysis was performed to collect CD data as a function of both focus and exposure for both photoresist products. Bossung plots for a 4 micron spacewidth in 10 microns of AZ P 4620 and STR 1075 are shown in figures 13 and 14 respectively. The AZ P 4620 results show a large variability in CD as a function of focus suggesting a poor process latitude. A narrow exposure range around 575 mJ/cm<sup>2</sup> appears to provide about 11 microns focus within a ±10% CD window. In contrast, the STR 1075 shows a very flat CD response across focus. Exposures ranging from 625 to 725 mJ/cm<sup>2</sup> provide greater than 16 microns depth of focus within a ±10% CD window.

### **DISCUSSION AND CONCLUSIONS**

TFH processing offers lithographic challenges just as severe as those encountered in submicron lithography for semiconductor manufacturing. The top pole level is a particularly challenging lithographic process. At that level, image aspect ratios frequently exceed 5:1 and the alignment in a thick photoresist film to the bottom pole is critical. Clearly, TFH lithography can benefit from process modeling to address these complex processing issues.

This study has demonstrated that the thick photoresist films used for TFH processing can be effectively modeled using lithography simulators such as PROLITH/2<sup>®</sup>. A full factorial design methodology has shown the importance of the photoresist absorption parameter **A** (μm<sup>-1</sup>) and the developer selectivity **n** in determining lithographic performance. High values of **n** provide increased process latitude while low values of **A** reduce the required exposure energy. Photoresist thicknesses effects were also studied and show that normalized process latitude decreases for extremely thick films. This appears to be a bulk absorption effect in combination with a developer loading phenomena.

Experimental results were obtained for two commercial photoresist products, Hoechst Celanese AZ 4000 and Shipley STR 1000. Develop rate results show a large difference in the **n** value between these two materials. The cross sectional SEM analysis and Bossung plots for 10 micron

films indicate that the STR 1000 family has a larger focus and exposure margin than AZ 4000. This supports the simulation predictions of the importance of developer selectivity  $n$  in lithographic performance.

## REFERENCES

1. Oshiki, M. and Hamasaki, S., "Thin-Film Head Technology", *Fujitsu Sci. Tech. J.*, Vol. 26 (4) February 1991, pp. 353-363.
2. Kryder, M.H., "Data-Storage Technologies for Advanced Computing", *Scientific American*, Vol. 257 (4), October 1987, pp. 117-125.
3. Ohdoi, Y. et. al., "A 48-Turn Thin Film Head for 150 Mb/in<sup>2</sup> Recording", *IEEE Transactions on Magnetics*, Vol. 26 (5), pp. 1671-1673.
4. Chapman, D. et. al., "A New Horizontal MR Head Structure", *IEEE Transactions on Magnetics*, Vol. 25 (5), pp. 3689-3691.
5. Gau, J.S., "Photolithography for Integrated Thin-Film Read/Write Heads", *Optical/ Laser Microlithography II*, Proc. SPIE Vol. 1088 (1989), pp. 504-514.
6. Flores, G., Flack, W., Dwyer, L., "Lithographic Performance of a New Generation i-line Optical System: A Comparative Analysis", *Optical/Laser Lithography VI*, Proc. SPIE Vol. 1927 (1993).
7. Mack, C. et. al., "Modeling and Characterization of a 0.5 mm Deep Ultraviolet Process", *J. Vac. Sci. Technol.*, B 9 (6) (1991), pp. 3143-3149.
8. Mack, C., "New Kinetic Model for Resist Dissolution", *J. Electrochem. Soc.*, 139 (4) (1992), pp. L35 - L37.
9. Box, G., Hunter, W., Hunter, J., *Statistics for Experimenters*, Wiley Interscience, John Wiley and Sons, New York (1978).
10. Trefonas, P., Mack, C., "Exposure Dose Optimization for a Positive Resist Containing Poly-functional Photoactive Compound", *Advances in Resist Technology and Processing VIII*, Proc., SPIE Vol. 1466 (1991) pp. 270 - 282.

Factor	Low	High
Absorption Parameter <b>A</b> ( $\mu\text{m}^{-1}$ )	0.4	1.1
Developer Selectivity <b>n</b>	1.5	6.0
Maximum Develop Rate <b>R<sub>max</sub></b> (nm/sec.)	50	200

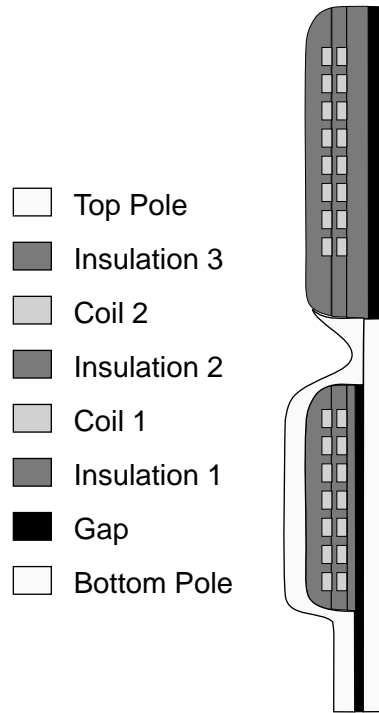
**TABLE 1.** Factorial design conditions used for process simulation studies.

Parameter	Setting
Optical System numerical aperture	0.24
Partial coherence	0.85
Illumination bandwidth nm	400 - 440
Photoresist parameter <b>A</b> ( $\mu\text{m}^{-1}$ )	<b>varied</b>
Photoresist parameter <b>B</b> ( $\mu\text{m}^{-1}$ )	0.05
Photoresist parameter <b>C</b> ( $\text{cm}^2/\text{mJ}$ )	0.016
Index of refraction	1.65
Substrate type	silicon
PEB Diffusion length	0
Maximum Develop Rate: <b>R<sub>max</sub></b> (nm/sec)	<b>varied</b>
Minimum Develop Rate: <b>R<sub>min</sub></b> (nm/sec)	0.1
Developer Selectivity <b>n</b>	<b>varied</b>
Threshold PAC concentration <b>m<sub>th</sub></b>	-10
Develop time (sec)	6* Photoresist thickness/ ( <b>R<sub>max</sub></b> )

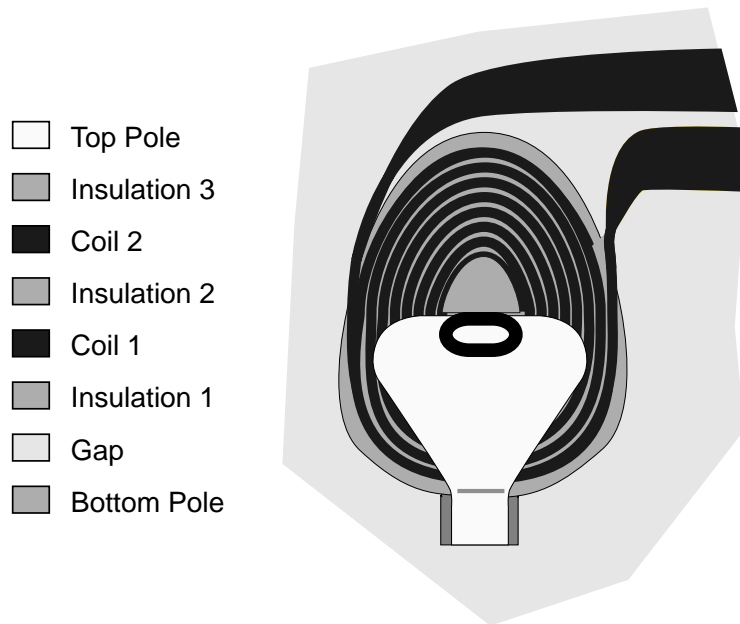
**TABLE 2.** Simulation parameter values held constant for process simulation studies.

A	n	Rmax	-3.3 microns defocus		-11.3 microns defocus	
			Exposure Latitude (%)	Sidewall Angle	Exposure Latitude (%)	Sidewall Angle
0.40	1.50	50	40	82	20	75
0.40	1.50	200	50	82	24	75
0.40	6.00	50	100	85	42	79
<b>0.40</b>	<b>6.00</b>	<b>200</b>	<b>140</b>	<b>85</b>	<b>57</b>	<b>79</b>
1.10	1.50	50	81	83	34	75
1.10	1.50	200	89	83	37	75
1.10	6.00	50	100	84	48	78
1.10	6.00	200	95	86	13	78

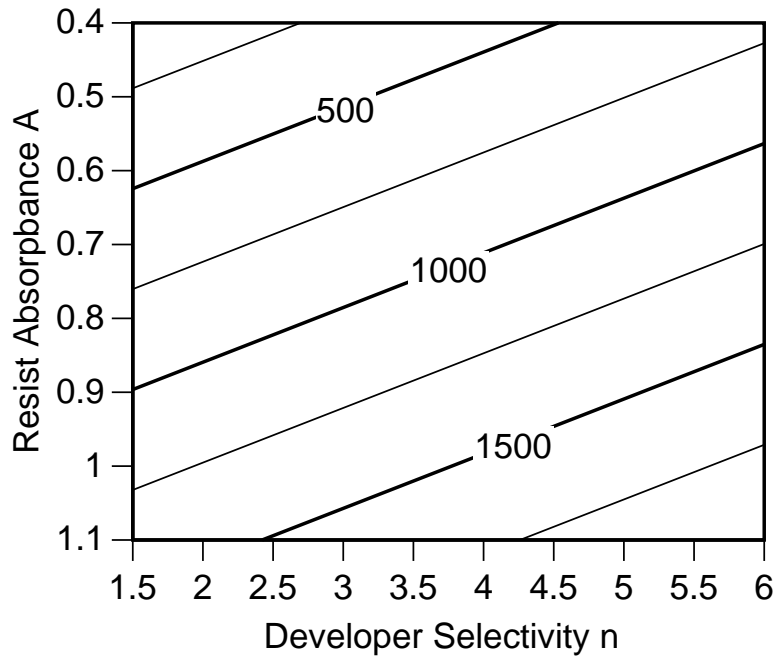
**TABLE 3.** Process response values from factorial design simulation.



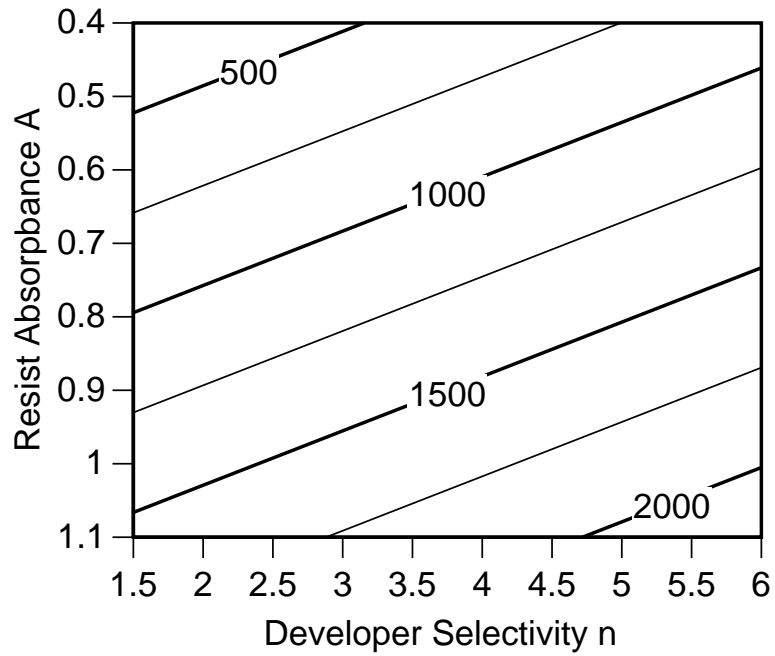
**FIGURE 1.** Cross section of a thin film head on a ceramic substrate. Typical geometries are six microns with greater than 20 microns of topography.



**FIGURE 2.** Top view of a thin film head on a ceramic substrate. Typical geometries are six microns with greater than 20 microns of topography.

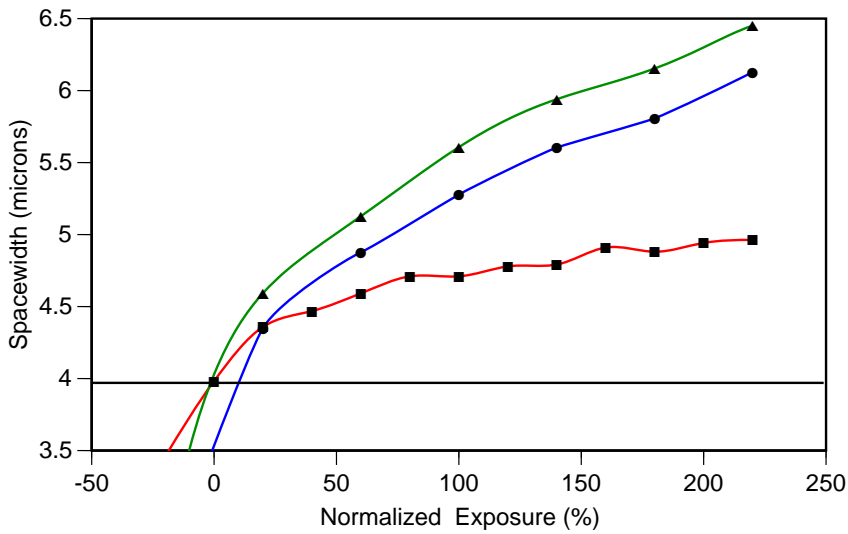


**FIGURE 3.** Contour plot of dose to size as a function of **A** and **n** for  $R_{\max}$  equal to 50.



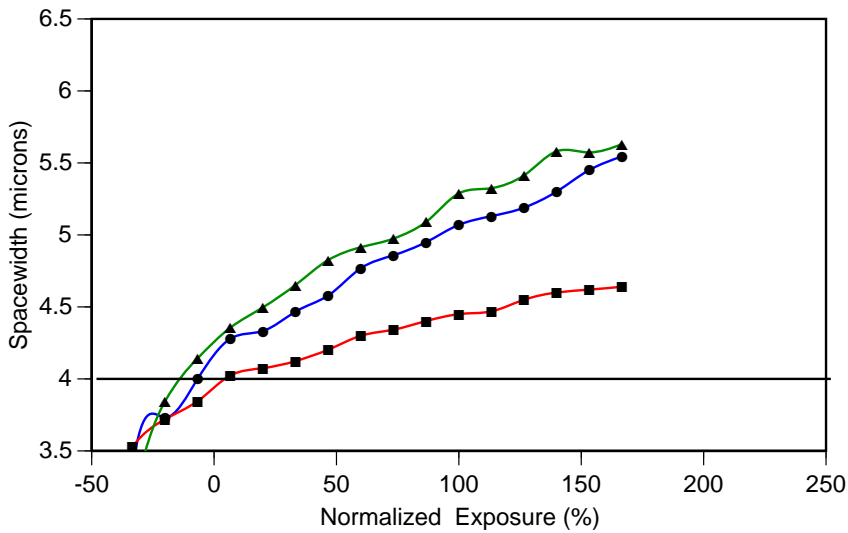
**FIGURE 4.** Contour plot of dose to size as a function of **A** and **n** for  $R_{\max}$  equal to 200.

Figure 5a



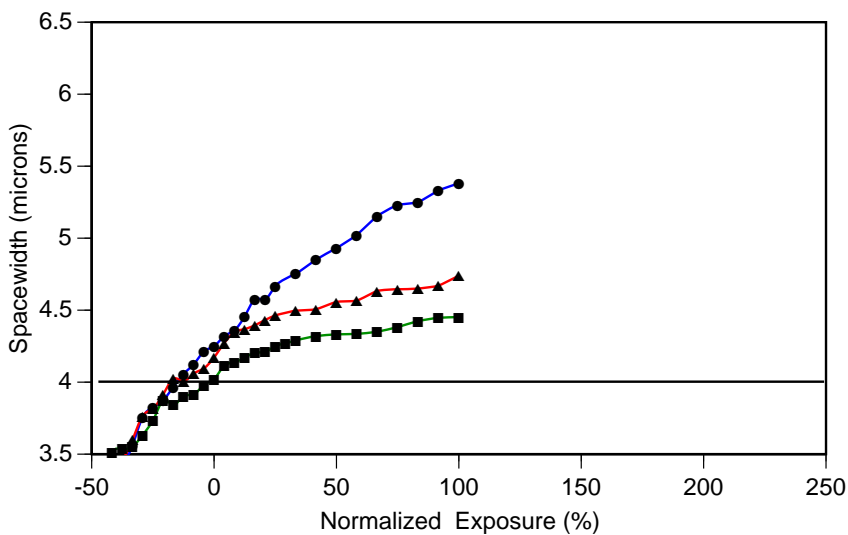
$A = 0.4 \text{ } (\mu\text{m}^{-1})$   
 $n = 1.5$   
 $R_{\text{max}} = 50 \text{ nm./sec.}$   
 Dose to size =  $250 \text{ mj/cm}^2$

Figure 5b



$A = 0.4 \text{ } (\mu\text{m}^{-1})$   
 $n = 6.0$   
 $R_{\text{max}} = 200 \text{ nm./sec.}$   
 Dose to size =  $750 \text{ mj/cm}^2$

Figure 5c

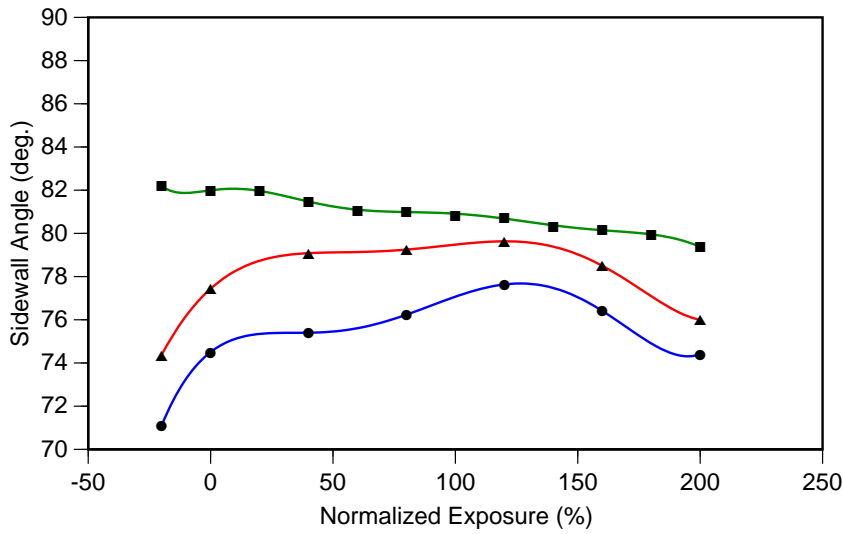


$A = 1.1 \text{ } (\mu\text{m}^{-1})$   
 $n = 6.0$   
 $R_{\text{max}} = 200 \text{ nm./sec.}$   
 Dose to size =  $2400 \text{ mj/cm}^2$

- Focus -11.3 microns
- ▲ Focus 4.7 microns
- Focus -3.3 microns

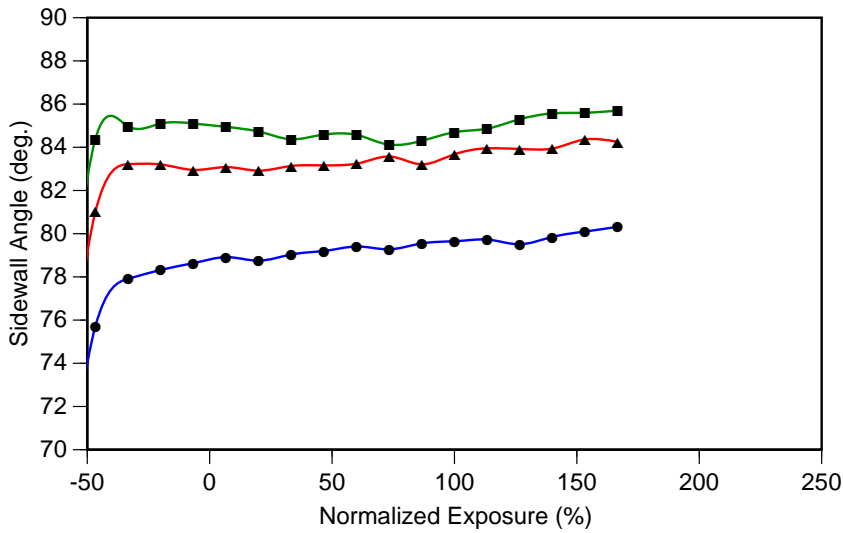
Figure 5. Simulation results of a 4 micron spacewidth versus normalized exposure dose through 16 microns defocus in a 10 micron photoresist film. Three different process conditions of  $A$ ,  $n$  and  $R_{\text{max}}$  are illustrated.

Figure 6a



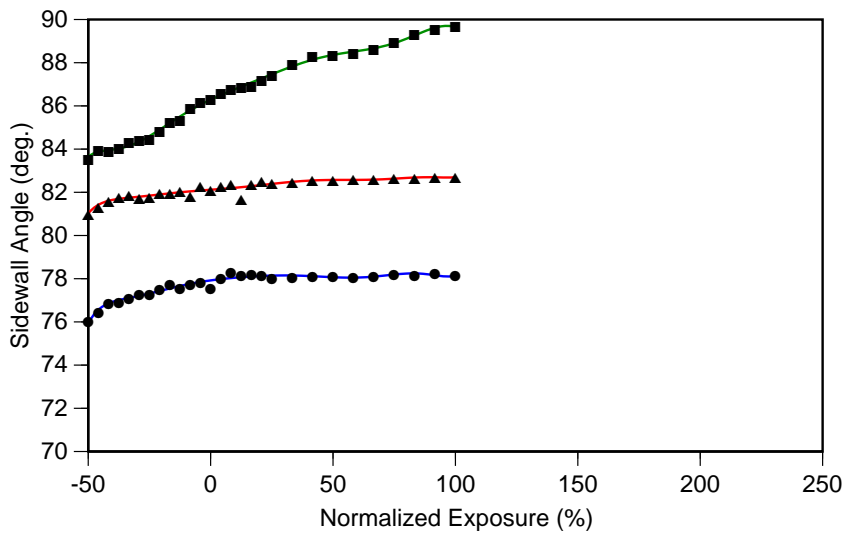
$A = 0.4 \text{ } (\mu\text{m}^{-1})$   
 $n = 1.5$   
 $R_{\text{max}} = 50 \text{ nm./sec.}$   
 Dose to size =  $250 \text{ mj/cm}^2$

Figure 6b



$A = 0.4 \text{ } (\mu\text{m}^{-1})$   
 $n = 6.0$   
 $R_{\text{max}} = 200 \text{ nm./sec.}$   
 Dose to size =  $750 \text{ mj/cm}^2$

Figure 6c



$A = 1.1 \text{ } (\mu\text{m}^{-1})$   
 $n = 6.0$   
 $R_{\text{max}} = 200 \text{ nm./sec.}$   
 Dose to size =  $2400 \text{ mj/cm}^2$

- Focus -11.3 microns
- ▲ Focus 4.7 microns
- Focus -3.3 microns

Figure 6. Simulation results of sidewall angle versus normalized exposure dose through 16 microns defocus in a 10 micron photoresist film. Three different process conditions of  $A$ ,  $n$  and  $R_{\text{max}}$  are illustrated for a 4 micron spacewidth.

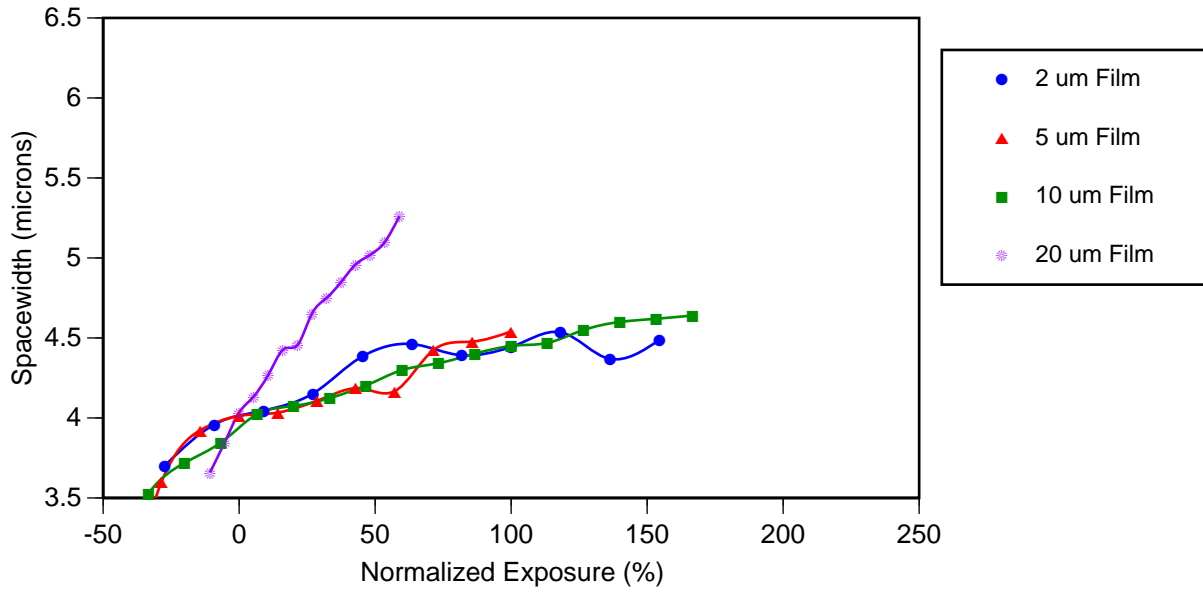


Figure 7. Simulation results of a 4 micron spacewidth versus normalized exposure (%) for film thickness of 2,5,10 and 20 microns.

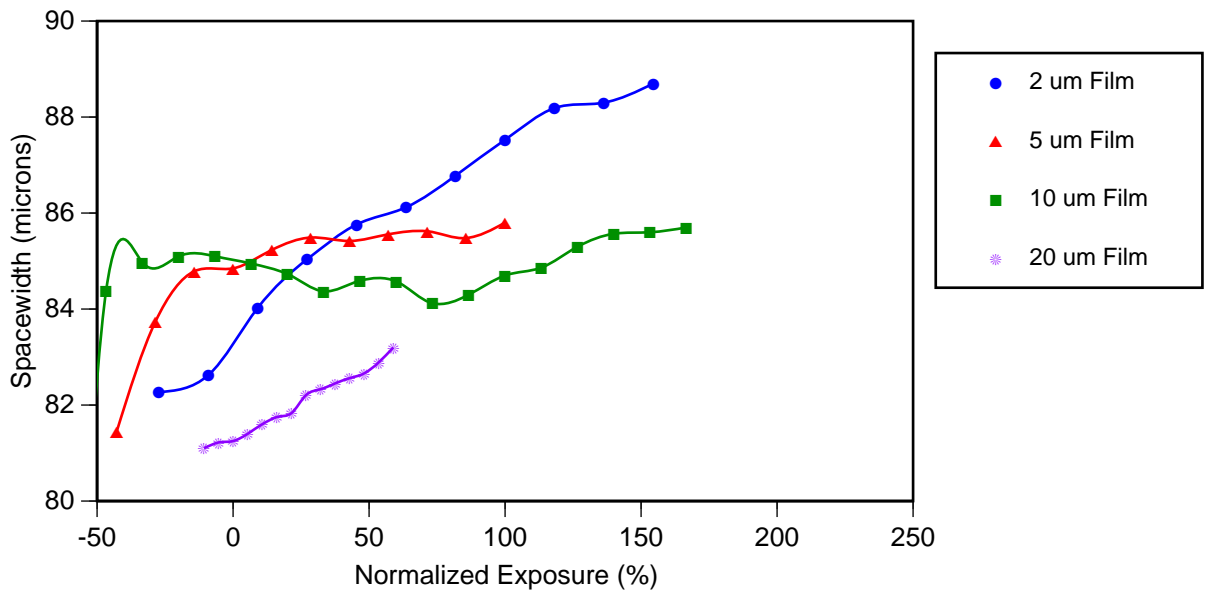


Figure 8 Simulation results of sidewall angle versus normalized exposure (%) for film thickness of 2,5,10 and 20 microns.

Figure 9a

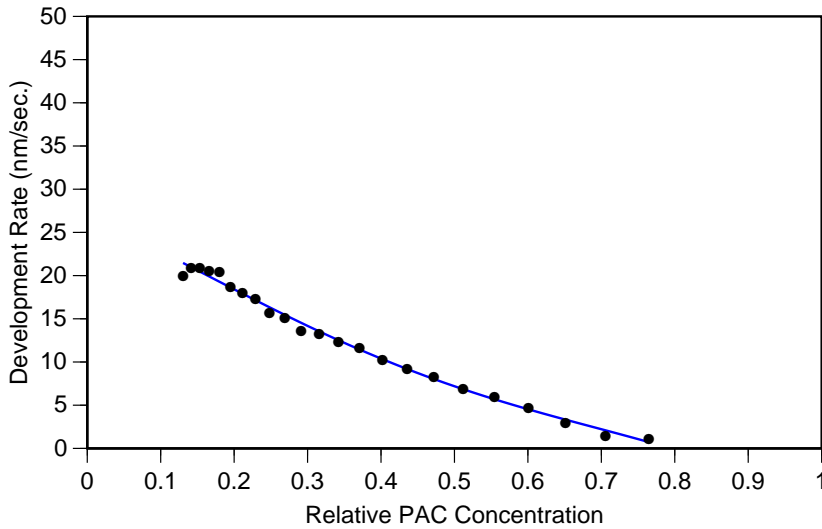


Figure 9b

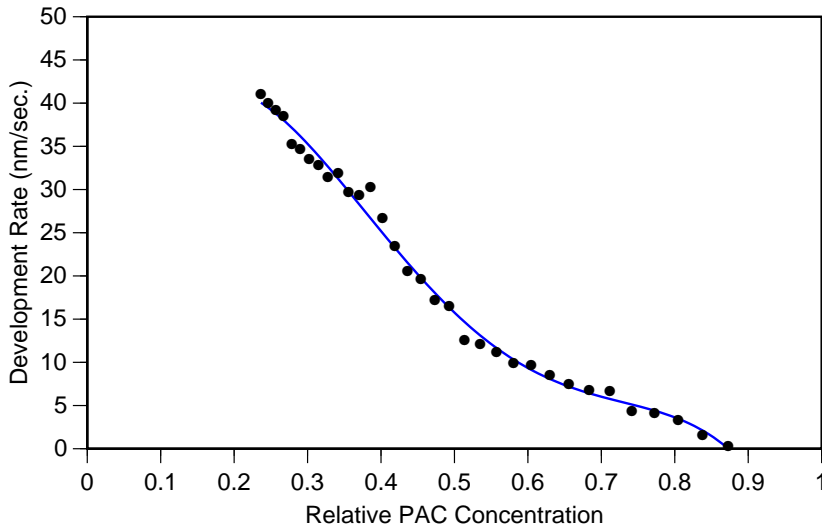


Figure 9c

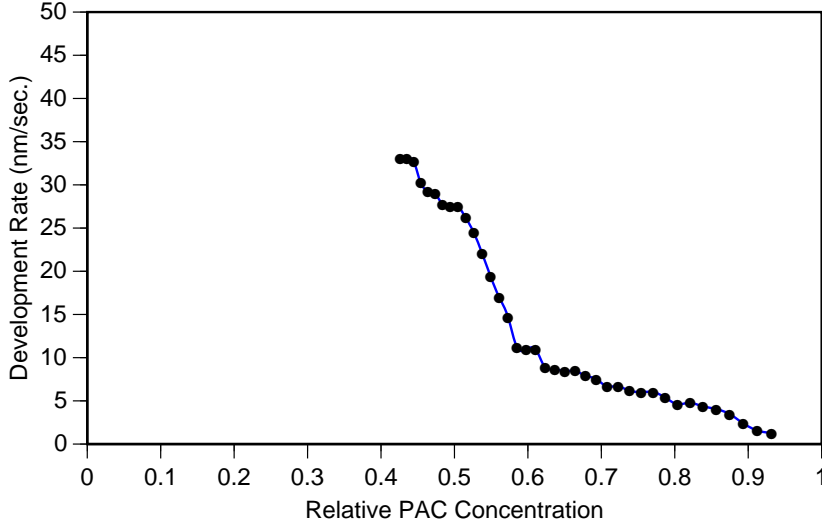
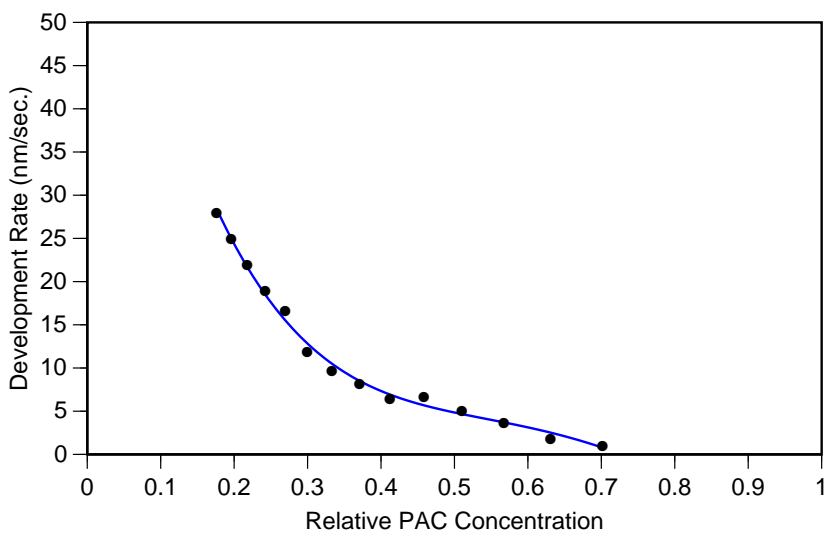


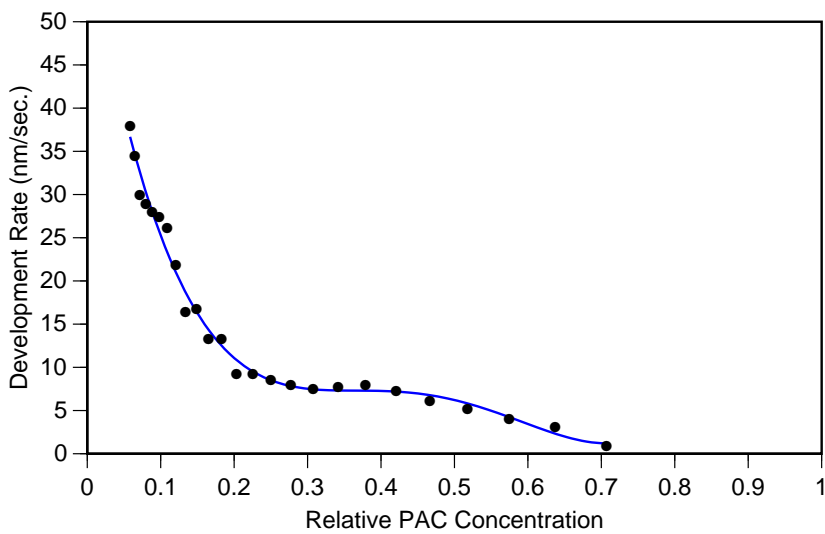
Figure 9. Plots of photoresist development rate versus relative PAC concentration and development rate parameters for AZ 4000 series photoresist at three different film thicknesses (top: 2 microns, center: 5 microns, bottom: 10 microns).

Figure 10a



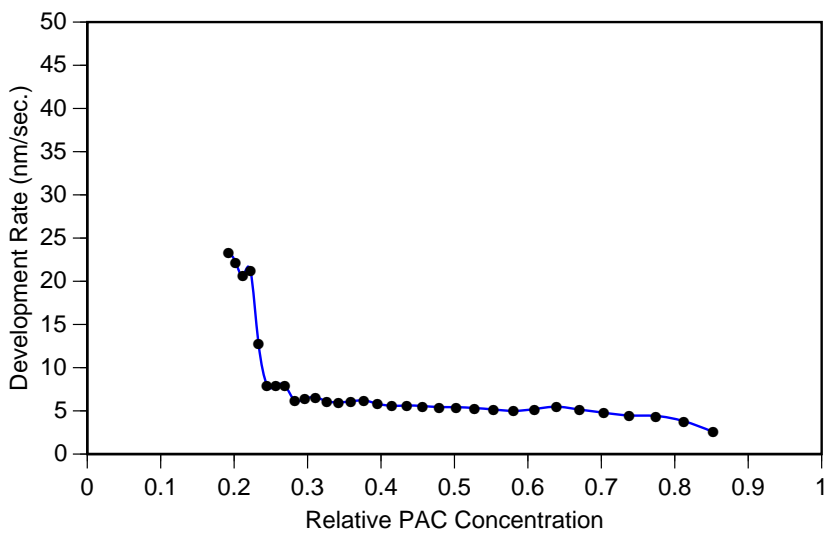
Shibley STR 1075  
2 micron film  
 $R_{max} = 63 \text{ nm./sec.}$   
 $R_{min} = 0.5 \text{ nm./sec.}$   
 $n = 4.4$

Figure 10b



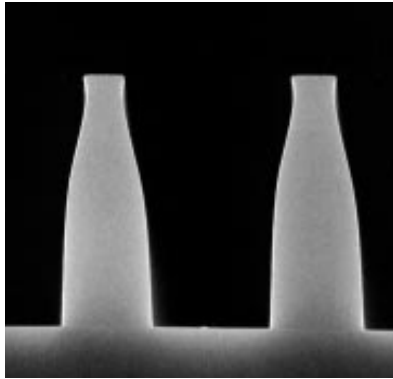
Shibley STR 1075  
5 micron film  
 $R_{max} = 55 \text{ nm./sec.}$   
 $R_{min} = 3 \text{ nm./sec.}$   
 $n = 5.0$

Figure 10c

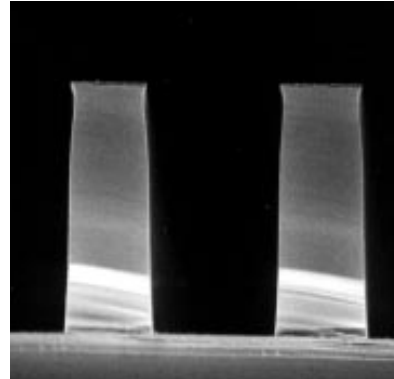


Shibley STR 1075  
10 micron film  
 $R_{max} = 75 \text{ nm./sec.}$   
 $R_{min} = 2 \text{ nm./sec.}$   
 $n = 4.5$

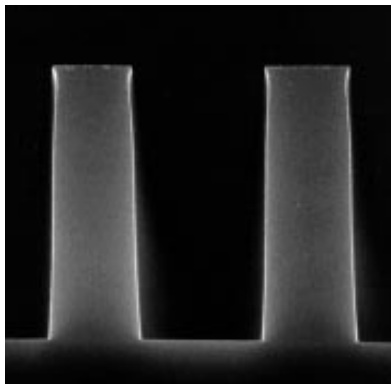
Figure 10. Plots of photoresist development rate versus relative PAC concentration and development rate parameters for Shibley STR 1075 series photoresist at three different film thicknesses (top: 2 microns, center: 5 microns, bottom: 10 microns).



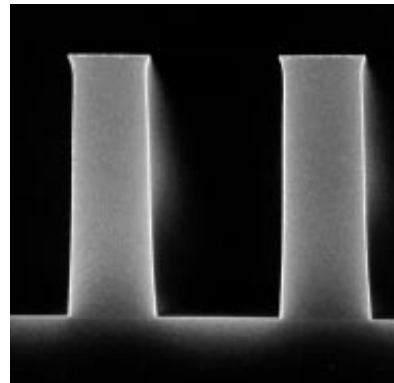
Focus -8.25  $\mu\text{m}$



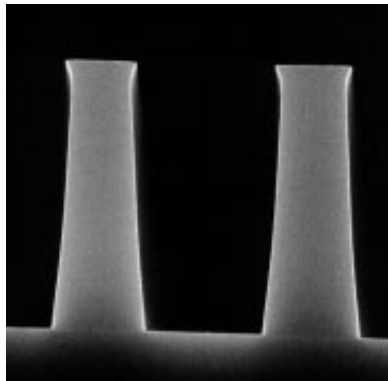
Focus -3.25  $\mu\text{m}$



Focus -2.00  $\mu\text{m}$

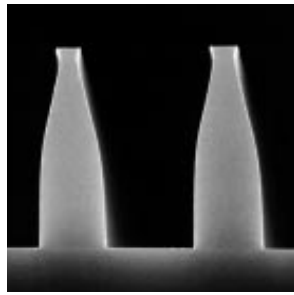


Focus -0.75  $\mu\text{m}$

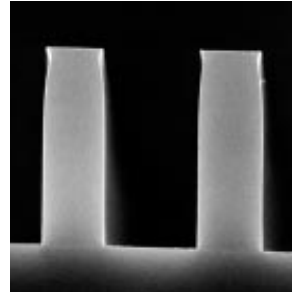


Focus +3.00  $\mu\text{m}$

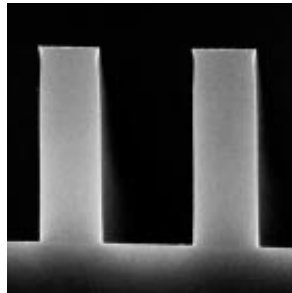
**Figure 11.** Depth-of-focus of 4 micron lines and spaces in 10 microns of AZ P4620 photoresist.



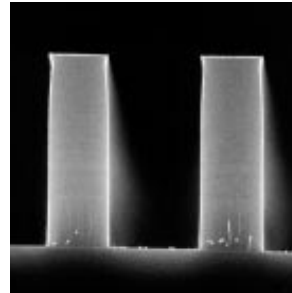
Focus -10.0  $\mu\text{m}$



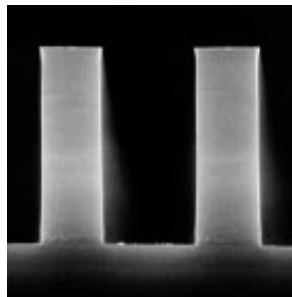
Focus -5.2  $\mu\text{m}$



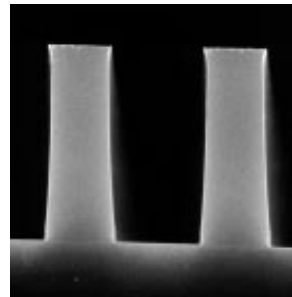
Focus -3.6  $\mu\text{m}$



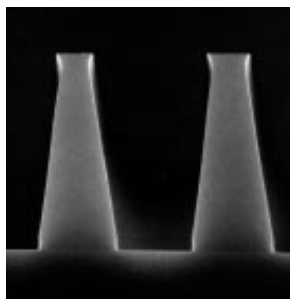
Focus -2.0  $\mu\text{m}$



Focus -0.4  $\mu\text{m}$



Focus +1.2  $\mu\text{m}$



Focus +6.0  $\mu\text{m}$

**Figure 12.** Depth-of-focus of 4 micron lines and spaces in 10 microns of STR 1075 photoresist.

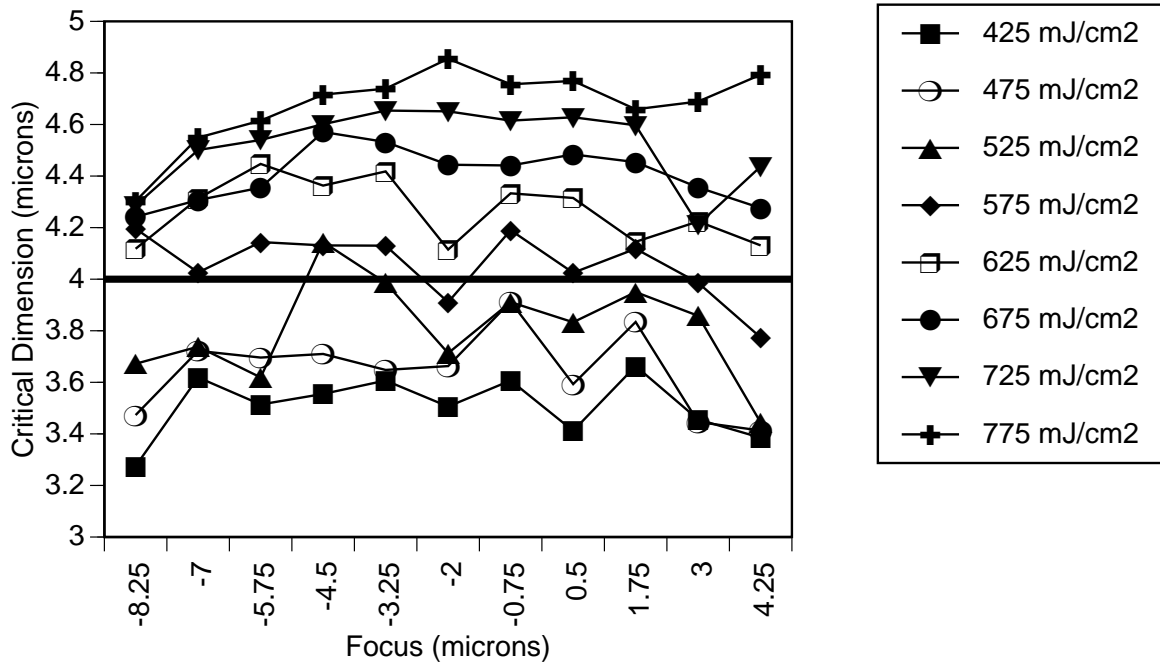


FIGURE 13. Bossung plot of 4 micron spacewidth in 10 microns of AZ P4620.

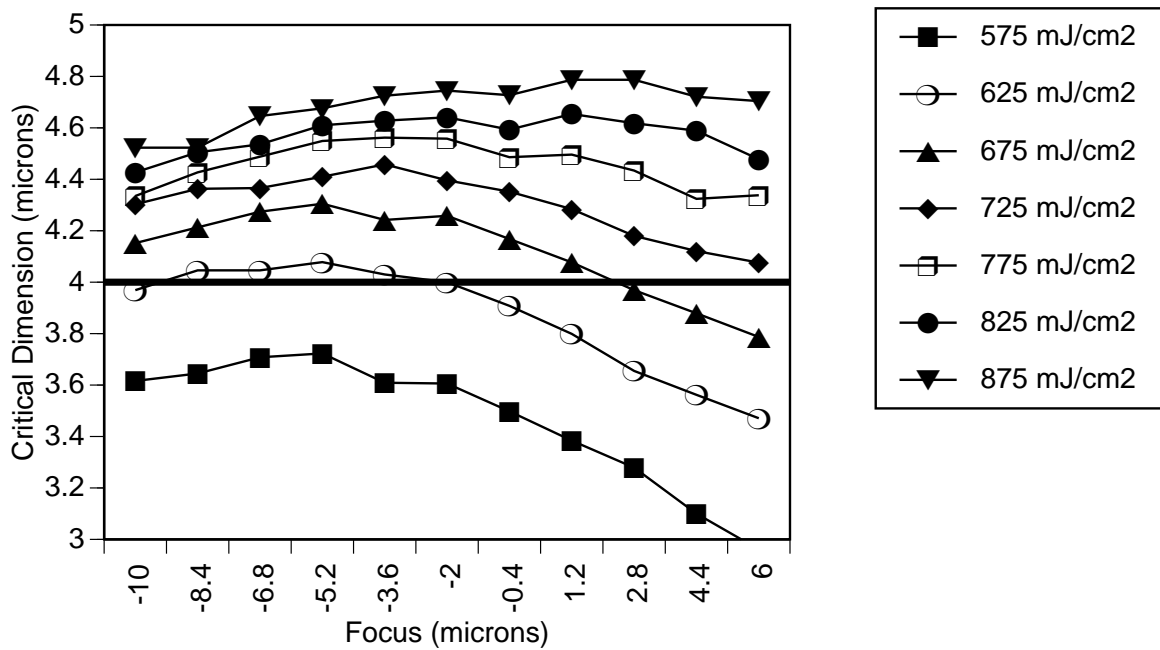


FIGURE 14. Bossung plot of 4 micron spacewidth in 10 microns of STR 1075.